Osteoarthritis and Cartilage 23 (2015) 661–670

Osteoarthritis and Cartilage

Cartilage-specific ablation of XBP1 signaling in mouse results in a chondrodysplasia characterized by reduced chondrocyte proliferation and delayed cartilage maturation and mineralization

T.L. Cameron †, I.L. Gresshoff †, K.M. Bell †, K.A. Piróg ‡, L. Sampurno †, C.L. Hartley §, E.M. Sanford †, R. Wilson †, J. Ermann ‖ ¶, R.P. Boot-Handford #, L.H. Glimcher ††, M.D. Briggs ‡, J.F. Bateman † ‡‡ *

† *Murdoch Childrens Research Institute, Parkville, Victoria, Australia*
‡ *Institute of Genetic Medicine, Newcastle University, International Centre for Life, Newcastle upon Tyne, UK*
§ *Central Manchester University Hospitals NHS Foundation Trust, St Mary's Hospital, Manchester, UK*
‖ *Division of Rheumatology, Immunology and Allergy, Brigham and Women's Hospital, Boston, MA, USA*
¶ *Harvard Medical School, Boston, MA, USA*
# *Wellcome Trust Centre for Cell-Matrix Research, Faculty of Life Sciences, The University of Manchester, Manchester, UK*
†† *Weill Cornell Medical College, Cornell University, New York, NY, USA*
‡‡ *Department of Biochemistry and Molecular Biology, University of Melbourne, Parkville, Victoria, Australia*

ARTICLE INFO

Article history:
Received 21 July 2014
Accepted 4 January 2015

Keywords:
Chondrodysplasia
Endochondral ossification
ER stress
Growth plate
XBP1

SUMMARY

Objective: To investigate the *in vivo* role of the IRE1/XBP1 unfolded protein response (UPR) signaling pathway in cartilage.
Design: *Xbp1*$^{flox/flox}$*.Col2a1-Cre* mice (*Xbp1*$^{Cart\Delta Ex2}$), in which XBP1 activity is ablated specifically from cartilage, were analyzed histomorphometrically by Alizarin red/Alcian blue skeletal preparations and X-rays to examine overall bone growth, histological stains to measure growth plate zone length, chondrocyte organization, and mineralization, and immunofluorescence for collagen II, collagen X, and IHH. Bromodeoxyuridine (BrdU) and terminal deoxynucleotidyl transferase dUTP nick end labeling (TUNEL) analyses were used to measure chondrocyte proliferation and cell death, respectively. Chondrocyte cultures and microdissected growth plate zones were analyzed for expression profiling of chondrocyte proliferation or endoplasmic reticulum (ER) stress markers by Quantitative PCR (qPCR), and of *Xbp1* mRNA splicing by RT-PCR to monitor IRE1 activation.
Results: *Xbp1*$^{Cart\Delta Ex2}$ displayed a chondrodysplasia involving dysregulated chondrocyte proliferation, growth plate hypertrophic zone shortening, and IRE1 hyperactivation in chondrocytes. Deposition of collagens II and X in the *Xbp1*$^{Cart\Delta Ex2}$ growth plate cartilage indicated that XBP1 is not required for matrix protein deposition or chondrocyte hypertrophy. Analyses of mid-gestation long bones revealed delayed ossification in *Xbp1*$^{Cart\Delta Ex2}$ embryos. The rate of chondrocyte cell death was not significantly altered, and only minimal alterations in the expression of key markers of chondrocyte proliferation were observed in the *Xbp1*$^{Cart\Delta Ex2}$ growth plate. IRE1 hyperactivation occurred in *Xbp1*$^{Cart\Delta Ex2}$ chondrocytes but was not sufficient to induce regulated IRE1-dependent decay (RIDD) or a classical UPR.
Conclusion: Our work suggests roles for XBP1 in regulating chondrocyte proliferation and the timing of mineralization during endochondral ossification, findings which have implications for both skeletal development and disease.

* Address correspondence and reprint requests to: J.F. Bateman, Murdoch Childrens Research Institute, Flemington Road, Parkville, Victoria 3052, Australia. Tel: 61-3-8341-6422.
E-mail addresses: trevor.cameron@mcri.edu.au (T.L. Cameron), irma.gresshoff@unimelb.edu.au (I.L. Gresshoff), katrina.bell@mcri.edu.au (K.M. Bell), katarzyna.pirog@newcastle.ac.uk (K.A. Piróg), lisa.sampurno@mcri.edu.au (L. Sampurno), claire.burgoyne@cmft.nhs.uk (C.L. Hartley), emma.sanford@mcri.edu.au (E.M. Sanford), richard.wilson@utas.edu.au (R. Wilson), jermann@partners.org (J. Ermann), ray.boot-handford@manchester.ac.uk (R.P. Boot-Handford), lglimche@med.cornell.edu (L.H. Glimcher), michael.briggs@newcastle.ac.uk (M.D. Briggs), john.bateman@mcri.edu.au (J.F. Bateman).

http://dx.doi.org/10.1016/j.joca.2015.01.001
1063-4584/

Introduction

Endochondral ossification is regulated in the cartilage growth plate, where chondrocytes secrete an elaborate extracellular matrix (ECM) and differentiate by proliferation and hypertrophy to drive longitudinal bone growth. Owing to the burden placed on the endoplasmic reticulum (ER) by the production of cartilage ECM components, chondrocytes rely on the unfolded protein response (UPR) to maintain ER homeostasis[1,2].

The UPR is regulated by ER membrane-spanning proteins including IRE1, ATF6, and PERK. These ER stress sensors reduce ER protein load by activating molecular pathways that increase the capacity of the ER to fold nascent proteins correctly and to eradicate chronically misfolded proteins, and reduce the overall rate of protein translation[3]. Several other ER sensors that are structurally and functionally homologous to ATF6 have also been described[1]. For cartilage development, the most important of these appears to be *BBF2H7*. Deletion of *Bbf2h7* causes a severe chondrodysplasia resulting from chondrocyte ER stress caused by impaired intracellular trafficking of secreted proteins[2]. Also important is ATF4, a transcription factor expressed following ER stress-induced activation of PERK. ATF4 controls chondrocyte proliferation and growth plate mineralization by regulating expression of IHH, and like BBF2H7 its ablation results in a dramatic chondrodysplasia[4]. Together these studies emphasize the importance of chondrocyte ER homeostasis for cartilage development. IRE1 signaling in cartilage development *in vivo* has not been investigated. IRE1 activation by ER stress results in the unconventional splicing of *XBP1* mRNA to encode a transcription factor that drives the expression of UPR target genes. IRE1 also acts independently of *XBP1* in a rapid response to ER stress known as regulated IRE1-dependent decay (RIDD), degrading a subset of transcripts encoding proteins normally processed via the ER[5].

XBP1 regulates several developmental processes involving professional secretory cells[6], and may also regulate cartilage development[7]. It was reported recently that spliced XBP1 ($XBP1_S$) was expressed in the mouse growth plate and during chondrogenic differentiation *in vitro*. Moreover, over-expression of $XBP1_S$ in these studies accelerated chondrocyte hypertrophy and the expression of *Ihh*, *Col10a1*, and *Runx2*, as well as *Pthrp*, while knockdown abolished hypertrophy and the expression of these genes. These data suggested that XBP1 may be required for chondrocyte hypertrophy by affecting IHH/PTHrP signaling and acting as a co-factor of RUNX2[7].

To determine if the XBP1 pathway controls chondrocyte hypertrophy *in vivo* we generated and characterized mice in which XBP1 was functionally inactivated by deletion of exon 2 in cartilage ($Xbp1^{CartΔEx2}$). We demonstrate that cartilage-specific ablation of XBP1 activity does not prevent chondrocyte hypertrophy *in vivo*, in contrast to predictions from *in vitro* data[7], but causes a chondrodysplasia phenotype involving shortening of endochondral bones and delayed endochondral ossification during development, but which resolves by skeletal maturity. Moreover $Xbp1^{CartΔEx2}$ growth plates are marked by shortening of the growth plate hypertrophic zone and dysregulated chondrocyte proliferation. This is the first study to implicate the IRE1/XBP1 signaling pathway in cartilage development *in vivo*, and suggests hitherto unknown physiological functions for IRE1/XBP1 signaling in development.

Methods

Generation of mice with cartilage-specific Xbp1 inactivation

Mice harboring *loxP* sites flanking exon 2 of *Xbp1*[8] were crossed with a transgenic mouse expressing Cre recombinase driven by the *Col2a1* promoter[9] to generate $Xbp1^{flox/flox}$.*Col2a1-Cre* ($Xbp1^{CartΔEx2}$), in which *Xbp1* mRNA is inactivated by Cre recombinase-mediated deletion of exon 2 in chondrocytes. *Xbp1* exon 2 deletion results in complete ablation of XBP1 protein but does not prevent IRE1-induced *Xbp1* mRNA splicing as an ER-stress reporter[10]. These mice were viable and bred normally, and were housed under pathogen-free conditions. Studies were performed with Institutional Ethics Committee approval and according to NIH guidelines for humane animal use. Genomic DNA (gDNA) was extracted by Proteinase K digestion of tail clips for genotyping, and purified by isopropanol precipitation. Genotyping was performed by PCR using primers to detect the presence of floxed *Xbp1* or *Col2a1*-Cre recombinase (PCR details available on request). To assess *Xbp1* inactivation in $Xbp1^{CartΔEx2}$ cartilage, RT-PCR was performed on wildtype and mutant epiphyseal cartilage cDNA with primers flanking *Xbp1* exon 2. PCR products were sequenced using the BigDye Terminator v3.1 Cycle Sequencing Kit (Life Technologies) to confirm deletion of *Xbp1* exon 2 in $Xbp1^{CartΔEx2}$ chondrocytes.

Skeletal preparations and morphometry

Mouse skeletons were analyzed morphometrically following Alcian blue and Alizarin red staining as described[11]. Femoral and tibial lengths were used to indicate endochondral bone growth, and intercanthal distance (ICD) to measure intramembranous bone growth[12]. X-ray images were prepared as described[12].

Immunofluorescence and histology

Immunofluorescence and histology was performed on PFA-fixed 10 μm cryosections or 5 μm paraffin-embedded sections of proximal tibial epiphyses from $Xbp1^{CartΔEx2}$ or wildtype mice. Immunofluorescence was performed using mouse anti-mouse collagen II (6B3, Neomarkers) rabbit anti-human collagen X, or rabbit anti-human IHH (EP1192Y, Abcam) and appropriate fluorescent secondary antibodies (10 μg/ml; Molecular Probes, Life Technologies). Rabbit polyclonal collagen X antibodies were produced using His_6-tagged full length human collagen X cDNA purified from transfected 293-EBNA cells[13]. Prior to antigen retrieval, all sections were incubated for 10 min at room temperature in PBS, 0.2% Triton X-100 (Sigma–Aldrich). For collagen II antigen retrieval, sections were digested for 10–15 min at 37°C in 2 mg/ml porcine pepsin (Sigma Aldrich). For collagen X antigen retrieval, sections were digested for 10–15 min at 37°C in 2 mg/ml bovine hyaluronidase (Sigma Aldrich). Collagen II staining was performed using reagents from the VECTOR M.O.M. Immunodetection Basic Kit (Vector Laboratories, Inc). All immunofluorescence sections were counterstained and mounted using VECTASHIELD Mounting Medium with DAPI (Vector Laboratories, Inc), and visualized using an Axio Imager M1 fluorescent microscope (Zeiss). Hematoxylin and eosin (H&E) staining was performed following a standard protocol involving staining in hematoxylin for 5 min and eosin for 1 min. Toluidine blue staining was performed using a standard protocol involving 10 min immersion in Toluidine blue and a 3 min counterstain in Fast Green. Staining for tissue mineralization was performed using standard protocols for Alizarin Red or Von Kossa stains.

Cell death and proliferation assays

Bromodeoxyuridine (BrdU) labeling analysis was performed by injecting Cell Proliferation Labeling Reagent (Amersham) peritoneally to detect growth plate chondrocyte proliferation[14]. Terminal deoxynucleotidyl transferase dUTP nick end labeling (TUNEL) was performed with the In Situ Cell Death Detection Kit, Fluorescein (Roche) to detect DNA fragmentation in cells undergoing programmed cell death[14].

Primary chondrocyte cultures

Primary chondrocytes from femoral and tibial condyles of 3 day old *Xbp1*^{CartΔEx2} mice were isolated as described[15] and cultured overnight at a concentration of approximately 1.0×10^5 cells/cm^2 in Dulbecco's modified Eagle's medium (DMEM), 10% fetal bovine serum (Thermo Fisher Scientific) supplemented with 1 mg/ml penicillin and 0.1 mg/ml streptomycin (Sigma Aldrich) at 37°C under 95% air, 5% CO_2. Media was replaced the following day with fresh media, with or without 2.5 ng/ml tunicamycin (Sigma Aldrich), and cultures were incubated for a further 4 h. RNA was extracted using the RNeasy Mini Kit (Qiagen).

Microdissection of growth plate zones, RNA isolation and amplification

Growth plate zones were microdissected from one proximal tibial growth plate from each of three 2 week old *Xbp1*^{CartΔEx2} and wildtype mice as described previously[16]. RNA was extracted from microdissected tissues using TRIzol reagent (Invitrogen). All total RNA samples were subjected to two rounds of linear amplification using the RNA ampULSe Amplification Kit (Kreatech). We have previously validated that this method preserves the relative abundance of transcripts present in cartilage total RNA samples[16–18]. Purity and integrity of all RNA samples were

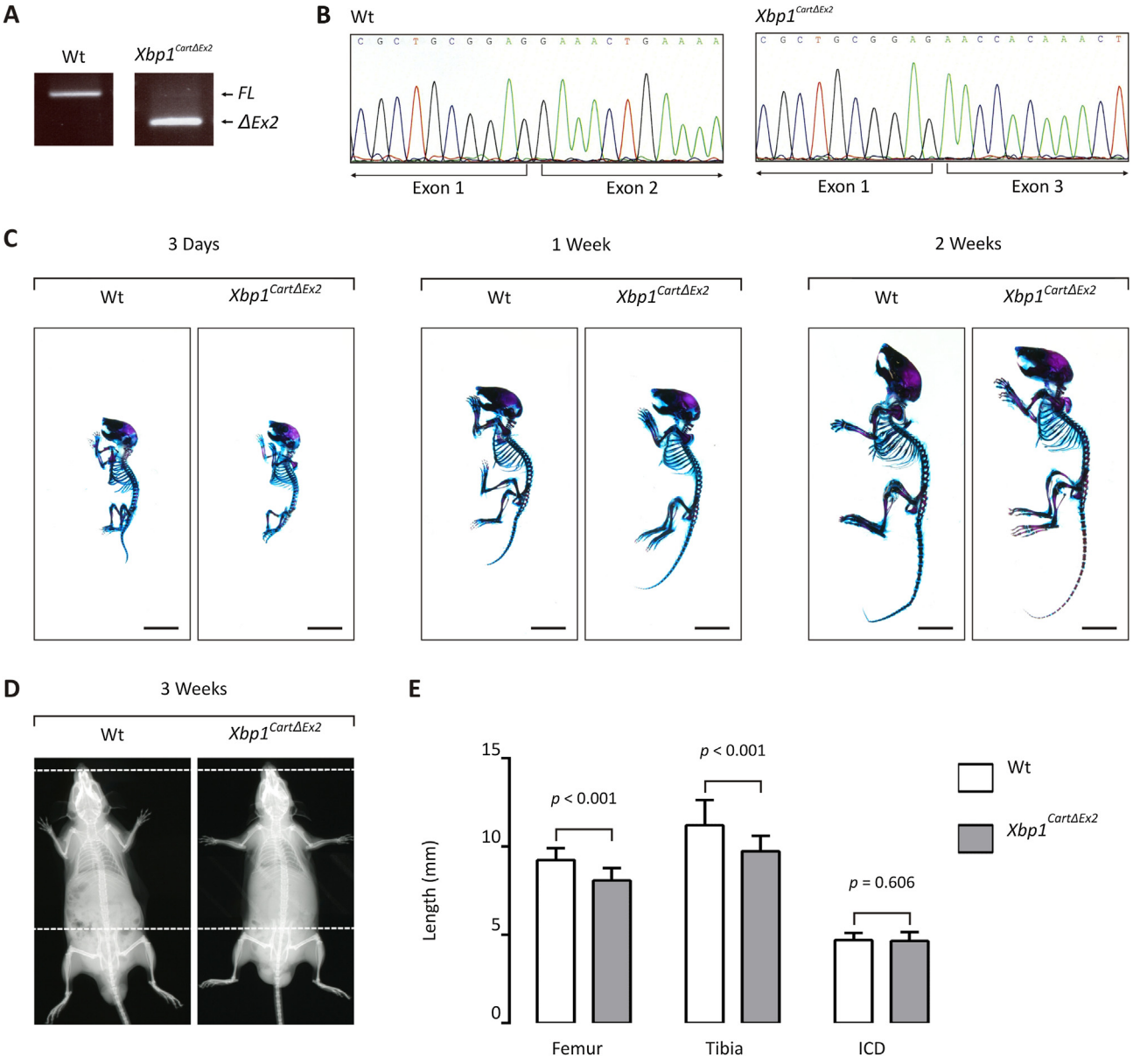

Fig. 1. Genetic and morphometric characterization of *Xbp1*^{CartΔEx2} mice. (A,B) cDNA from wildtype (Wt) and *Xbp1*^{CartΔEx2} femoral head cartilage analyzed by (A) RT-PCR to detect the full-length form of *Xbp1* (FL) or the inactive form of *Xbp1* lacking exon 2 (*ΔEx2*), and (B) sequencing to confirm the deletion of exon 2 from *Xbp1* in *Xbp1*^{CartΔEx2} cartilage. (C,D) Overall skeletal development assessed by (C) whole mount Alizarin red S/Alcian blue staining of skeletal preparations from 3 day old, 1 week, and 2 week Wt and *Xbp1*^{CartΔEx2} mice, and (D) X-ray analysis of 3 week Wt and *Xbp1*^{CartΔEx2} mice. (E) Measurements of femoral and tibial length, and intercanthal distance (ICD) from 2 week Wt and *Xbp1*^{CartΔEx2} mice – Wt, $N = 8$; *Xbp1*^{CartΔEx2}, $N = 9$.

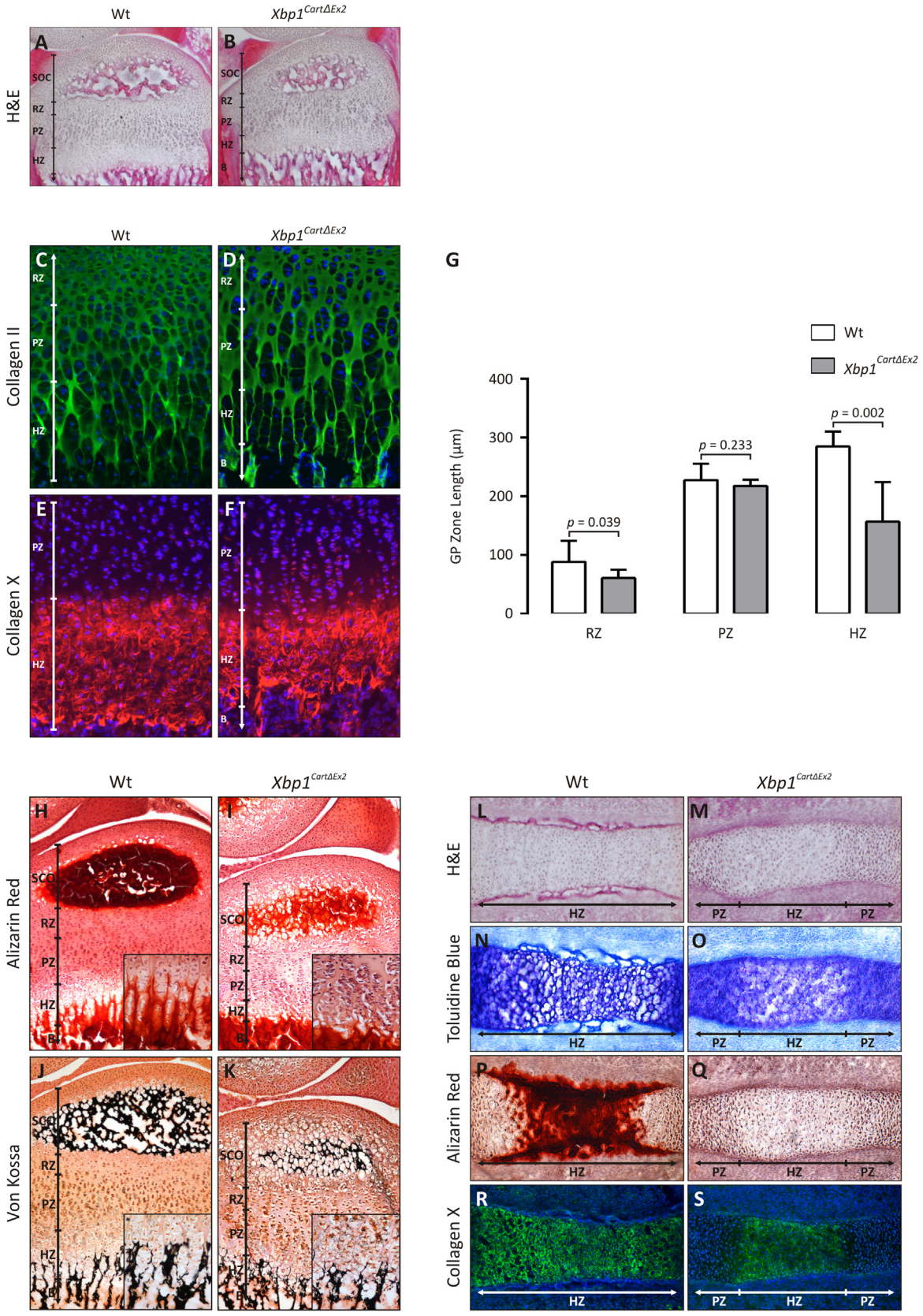

Fig. 2. XBP1 controls growth plate structure and mineralization. (A–F) Tibial epiphyseal cryosections from 2 week wildtype (Wt) and *Xbp1*^{CartΔEx2} mice stained (A,B) with hematoxylin and eosin (H&E) and by immunofluorescence for (C,D) collagen II and (E,F) collagen X. (G) Quantitative analysis of growth plate zone lengths from H&E-stained tibial cryosections of 2 week Wt and *Xbp1*^{CartΔEx2} mice. (H–K) Tibial epiphyseal cryosections from 2 week Wt and *Xbp1*^{CartΔEx2} mice stained with (H,I) Alizarin Red or (J,K) Von Kossa stain. (L–S) Tibial cryosections from E15.5 Wt and *Xbp1*^{CartΔEx2} embryos stained with (L,M) H&E, (N,O) Toluidine Blue, (P,Q) Alizarin Red, or (R,S) by immunofluorescence for collagen X. B – bone, HZ – hypertrophic zone, PZ – proliferative zone, RZ – resting zone, SCO – secondary center of ossification.

validated by electrophoresis with a 2200 TapeStation using a High Sensitivity R6K Screen Tape Kit (Agilent Technologies).

Quantitative PCR (qPCR) analysis

For *Xbp1* splicing, RT-PCR was performed on equal quantities of cDNA using primers flanking the ER stress-responsive *Xbp1* splice site. qPCR was performed on equal quantities of cDNA using the LightCycler 480 Probes Master Kit on a LightCycler 480 II qPCR machine (Roche Applied Science) as described[16]. All primer sequences are available on request.

Statistical methods

All quantitative data were generated using biological replicates in triplicate, unless stated otherwise, and are expressed as the mean plus 95% confidence interval. In each case, *P* values were determined using the unpaired Student's *t* test. All analyses were conducted using GraphPad QuickCalcs software (La Jolla, CA, USA).

Results

$Xbp1^{Cart\Delta Ex2}$ mice exhibit mild dwarfism and delayed ossification

RT-PCR analysis and sequencing confirmed deletion of exon 2 from *Xbp1* mRNA in $Xbp1^{Cart\Delta Ex2}$ but not wildtype cartilages [Fig. 1(A),(B)]. When $Xbp1^{Cart\Delta Ex2}$ and wildtype mice were compared by Alcian blue/Alizarin red staining of skeletal preparations or X-rays, the mutants exhibited mild dwarfism [Fig. 1(C),(D)]. At 2 weeks of age, endochondral bones in mutant mice were shortened by approximately 13% compared with wildtype, but no difference was observed in ICD between mutant and wildtype [Fig. 1(E)], indicating that intramembranous bone formation was unaffected. By 7 weeks of age, no difference was observed between wildtype and $Xbp1^{Cart\Delta Ex2}$ in the length of endochondral bones (Fig. S1(A)). Thus $Xbp1^{Cart\Delta Ex2}$ mice exhibited a mild chondrodysplasia during development that resolved by skeletal maturity.

Histological analysis of endochondral ossification revealed important clues to the $Xbp1^{Cart\Delta Ex2}$ phenotype. H&E staining of 2 week growth plates suggested delayed development of the secondary ossification center and hypertrophic zone shortening in mutant vs wildtype [Fig. 2(A),(B)]. Hypertrophic zone shortening was confirmed by collagen X immunofluorescence in adult [Fig. 2(E),(F)] and embryonic tissues [Fig. 2(R),(S)]. Growth plate zone lengths were also quantified in 2 week old mice using H&E-stained tissues. This revealed an approximately 45% reduction in hypertrophic zone length and a modest reduction in resting zone length in $Xbp1^{Cart\Delta Ex2}$ vs wildtype at 2 weeks of age [Fig. 2(G)]; no differences were apparent in growth plate zone length between wildtype and mutant at 7 weeks of age (Fig. S1(B)). Delayed mineralization of $Xbp1^{Cart\Delta Ex2}$ endochondral bones during development was confirmed in 2 week old [Fig. 2(H)–(K)] and embryonic tissues [Fig. 2(P),(Q)] by Alizarin Red or Von Kossa staining. Finally, that no apparent difference in the secretion or deposition of either collagen II or collagen X was apparent by immunofluorescent analysis of $Xbp1^{Cart\Delta Ex2}$ cartilage vs wildtype [Fig. 2(C)–(F)] suggests that neither cartilage matrix assembly, nor chondrocyte hypertrophy depend on XBP1 signaling in cartilage development.

Chondrocyte proliferation is dysregulated in the $Xbp1^{Cart\Delta Ex2}$ growth plate but cell death is not

H&E staining of 2 week tibial growth plate sections revealed architectural differences between the $Xbp1^{Cart\Delta Ex2}$ and wildtype proliferative zones, with longer chondrocyte columns and increased prevalence and size of areas of hypocellularity in the

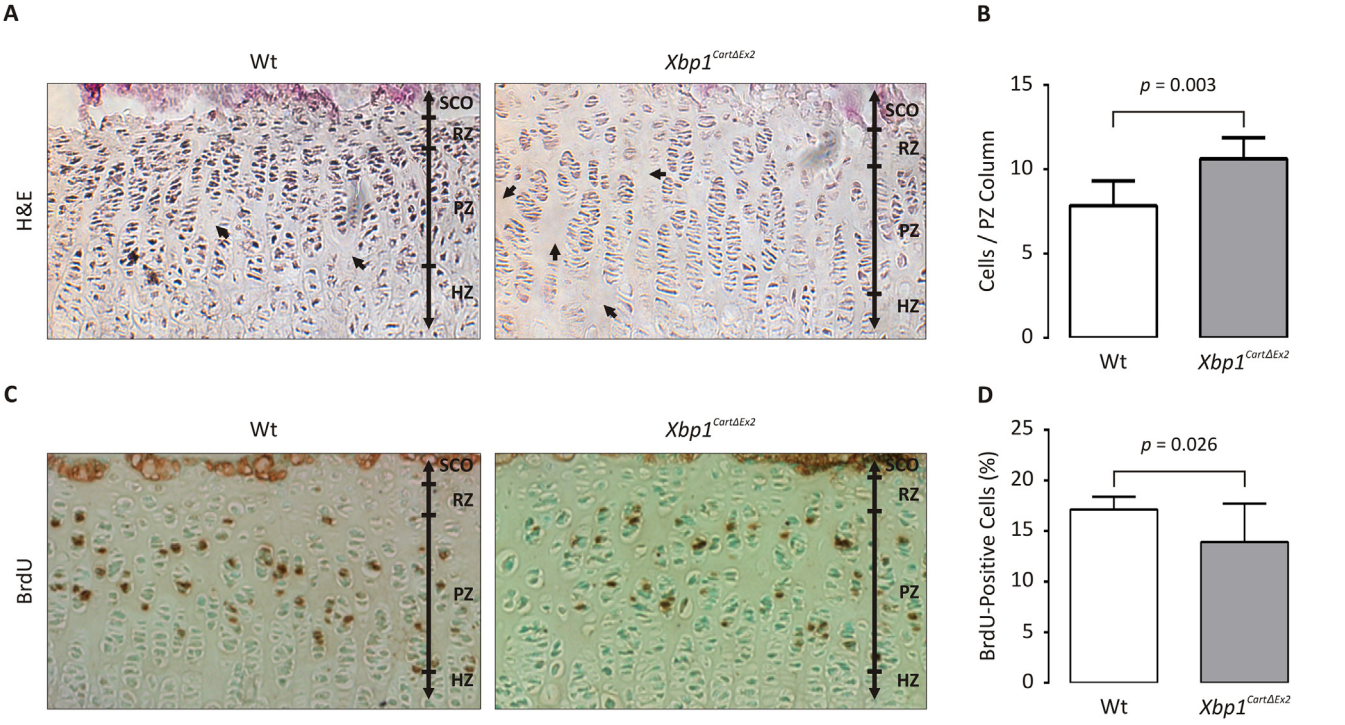

Fig. 3. XBP1 regulates proliferative zone architecture and chondrocyte proliferation. (A) Representative images of hematoxylin and eosin (H&E) staining to assess chondrocyte column length in wildtype (Wt) and $Xbp1^{Cart\Delta Ex2}$ proliferative zones. Arrows in (A) indicate areas of hypocellularity. (B) Quantification of chondrocyte column length analysis represented in (A). (C) Representative images of BrdU analysis to assess chondrocyte proliferation in Wt and $Xbp1^{Cart\Delta Ex2}$ growth plates. (D) Quantification of BrdU analysis represented in (C). HZ – hypertrophic zone, PZ – proliferative zone, RZ – resting zone, SCO – secondary center of ossification.

mutant vs wildtype, indicating dysregulated chondrocyte proliferation in the mutant [Fig. 3(A),(B)]. BrdU analysis of *Xbp1*^{CartΔEx2} and wildtype growth plates demonstrated a modest reduction in chondrocyte proliferation in the *Xbp1*^{CartΔEx2} proliferative zone compared with wildtype ($P = 0.026$; Fig. 3(C),(D)).

To investigate the proliferative defect at the transcriptional level, we microdissected proliferative and hypertrophic zones from *Xbp1*^{CartΔEx2} and wildtype mice. Expression profiling was performed by qPCR for the following genes implicated in chondrocyte proliferation: *Atf2*[19], *Atf3*[20], *Ccna2*[21], *Ccnd1*[22], *Fgfr3*[23], and *Ihh*, which regulates chondrocyte proliferation from its site of expression in the hypertrophic zone[24] [Fig. 4(A)–(F)]. None of these genes were differentially expressed between *Xbp1*^{CartΔEx2} and wildtype except for *Ccnd1*, which appeared to be upregulated approximately 2-fold in the proliferative zone of *Xbp1*^{CartΔEx2} compared to wildtype ($P = 0.038$). Since IHH regulates both chondrocyte proliferation and bone collar formation[25], both of which were dysregulated in *Xbp1*^{CartΔEx2}, we confirmed IHH expression in the mutant by immunofluorescence [Fig. 4(G)–(J)]. IHH was detected at comparable levels in proliferating chondrocytes in wildtype vs mutant in both E15.5 tibiae and 2 week tibial growth plates. IHH was also detected in the developing bone collar of wildtype E15.5 tibiae, which was absent from E15.5 *Xbp1*^{CartΔEx2} tibiae.

TUNEL analysis was performed on *Xbp1*^{CartΔEx2} and wildtype growth plates (Fig. S2) to examine chondrocyte cell death in the mutants. No significant changes in the ratio of TUNEL-positive cells:DAPI-stained nuclei were apparent in the *Xbp1*^{CartΔEx2} resting, proliferative, or hypertrophic zones by comparison with their corresponding wildtype zones. Thus cell death is unlikely to contribute to the mutant phenotype.

A classical UPR is not activated in the Xbp1^{CartΔEx2} *growth plate*

We investigated the UPR in *Xbp1*^{CartΔEx2} chondrocytes by testing their response to ER stress *in vitro*, and by performing expression profiling using the microdissected *Xbp1*^{CartΔEx2} and wildtype growth plate zones (Fig. 5). Increased *Xbp1* splicing and *BiP* upregulation were observed in primary *Xbp1*^{CartΔEx2} chondrocytes cultured in tunicamycin compared to control cultures, demonstrating that the UPR is not intrinsically compromised in *Xbp1*^{CartΔEx2} cartilage [Fig. 5(A),(B)]. In the growth plate, sentinel markers of the chondrocyte UPR[16] were examined. *BiP* was modestly upregulated in the

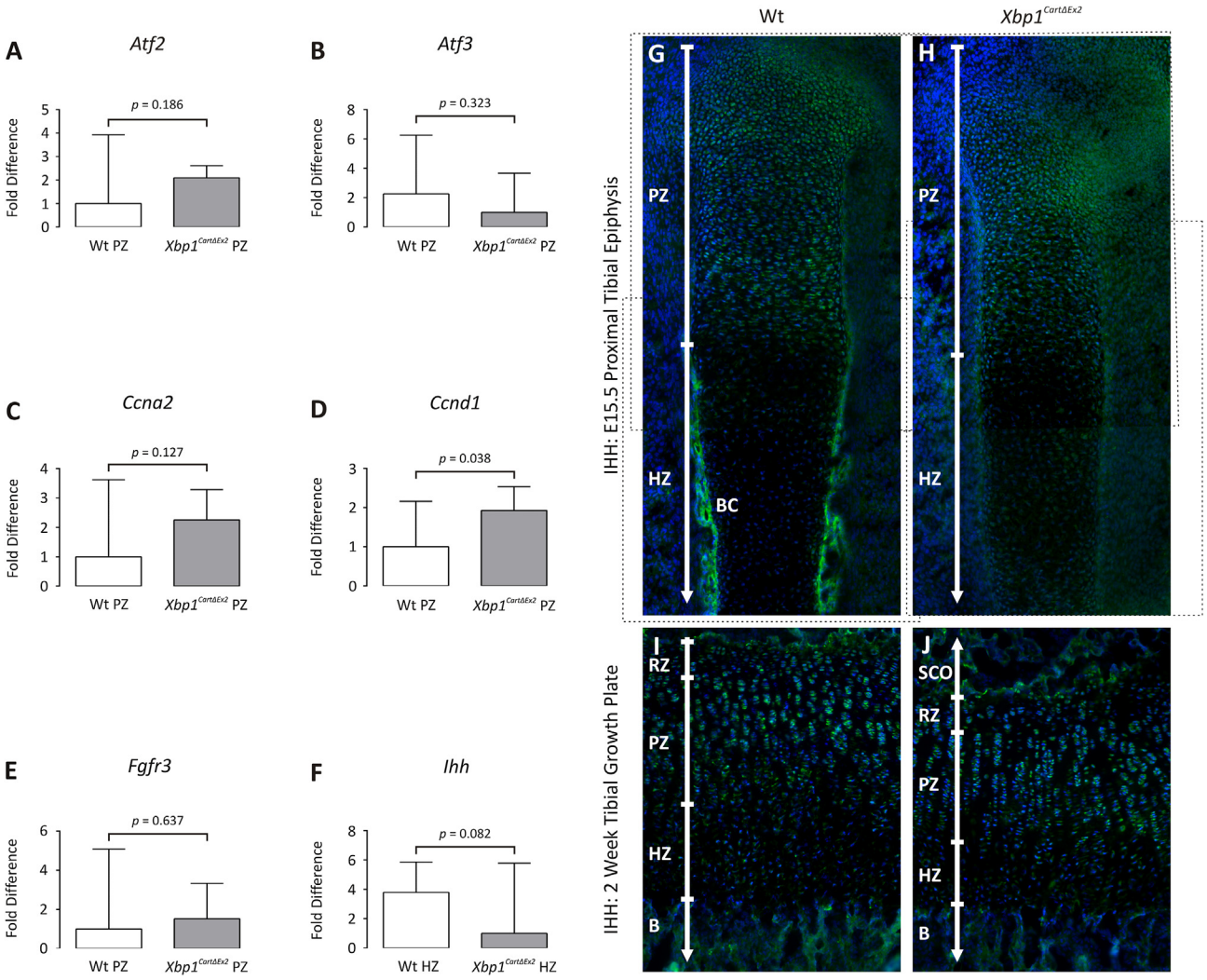

Fig. 4. Expression profiling of chondrocyte proliferation markers in developing Wt and *Xbp1*^{CartΔEx2} long bones. (A–F) qPCR performed on cDNA derived from microdissected wildtype (Wt) and *Xbp1*^{CartΔEx2} growth plate zones as indicated, using primers specific for (A) *Atf2*, (B) *Atf3*, (C) *Ccna2*, (D) *Ccnd1*, (E) *Fgfr3*, and (F) *Ihh*. (G–J) IHH immunofluorescence in (G,H) E15.5 Wt and *Xbp1*^{CartΔEx2} proximal tibial epiphyses, and in (I,J) two week Wt and *Xbp1*^{CartΔEx2} tibial growth plates. Dashed lines in (G) and (H) indicate relative positions of original images used to generate composite images as shown. B – bone, BC – bone collar, HZ – hypertrophic zone, PZ – proliferative zone, RZ – resting zone, SCO – secondary center of ossification.

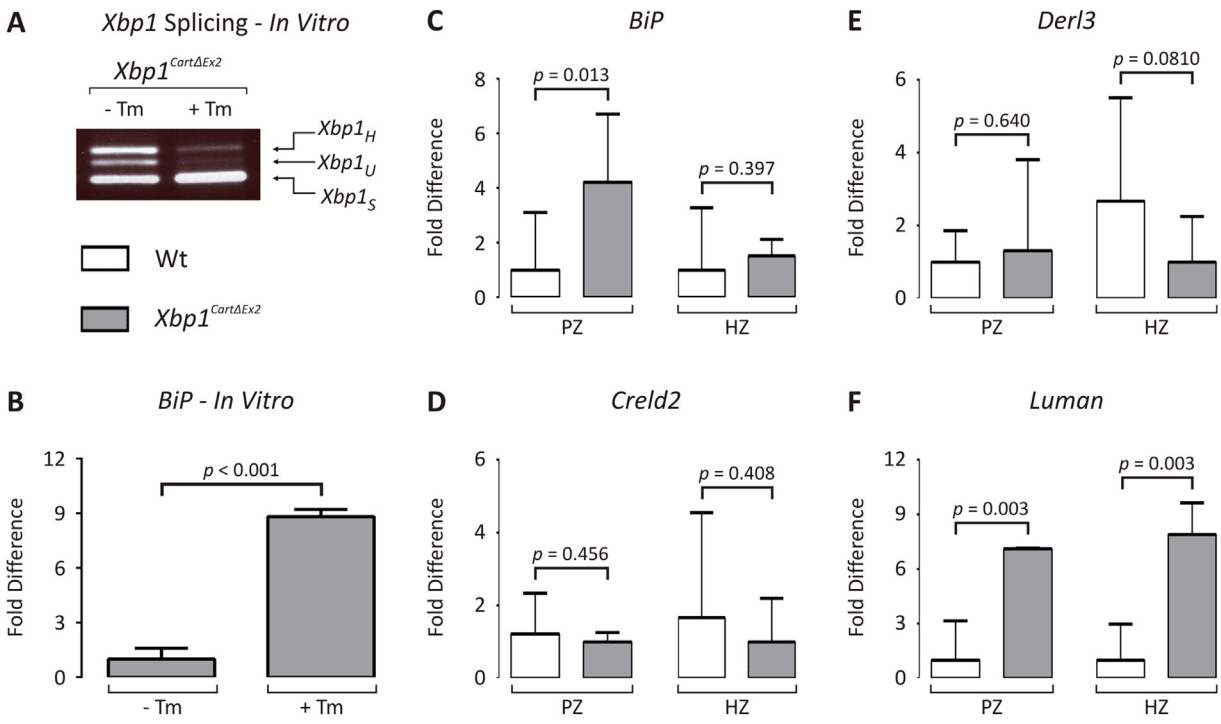

Fig. 5. XBP1 is not required by chondrocytes to maintain ER homeostasis. (A) RT-PCR performed on cDNA derived from primary *Xbp1*^{CartΔEx2} chondrocytes following culture with (+Tm) or without (−Tm) tunicamycin to detect the unspliced (*Xbp1*$_U$) and spliced (*Xbp1*$_S$) forms of *Xbp1* in response to ER stress. *Xbp1*$_H$ denotes a heteroduplex product comprised of both *Xbp1*$_U$ and *Xbp1*$_S$ strands. (B) qPCR performed on the +Tm and −Tm cDNA described in (A) to assess differential expression of *BiP* in *Xbp1*^{CartΔEx2} cartilage following induction of ER stress. (C–F) qPCR performed on cDNA derived from microdissected wildtype (Wt) and *Xbp1*^{CartΔEx2} growth plate zones, using primers specific for (C) *BiP*, (D) *Creld2*, (E) *Derl3*, and (F) *Luman*. PZ – proliferative zone, HZ – hypertrophic zone.

Xbp1^{CartΔEx2} proliferative zone vs wildtype ($P = 0.013$) but not the hypertrophic zone [Fig. 5(C)]. Differential expression was not observed however for *Creld2* [Fig. 5(D)] or *Derl3* [Fig. 5(E)] in either zone between mutant and wildtype. *Luman* was upregulated in *Xbp1*^{CartΔEx2} vs wildtype in both the proliferative and hypertrophic zones [Fig. 5(F)]. Thus *Xbp1*^{CartΔEx2} chondrocytes can respond to ER stress, however ablation of XBP1 activity does not result in activation of a classical UPR *in vivo*.

IRE1 is hyperactivated in the Xbp1^{CartΔEx2} *growth plate but does not cause RIDD*

Xbp1 splicing analysis of *Xbp1*^{CartΔEx2} primary chondrocytes indicated that significant *Xbp1* splicing occurs in untreated cells [Fig. 5(A)], revealing that IRE1 hyperactivation via a feedback loop previously reported in XBP1-deficient pancreatic β-islet cells[26] also occurs in *Xbp1*^{CartΔEx2} chondrocytes *in vitro*. To confirm whether IRE1 is hyperactivated in the *Xbp1*^{CartΔEx2} growth plate, we investigated *Xbp1* splicing in *Xbp1*^{CartΔEx2} and wildtype growth plate zones [Fig. 6(A)]. In the wildtype proliferative zone, most *Xbp1* transcripts were *Xbp1*$_U$, however low levels of *Xbp1*$_S$ were also detectable. In the wildtype hypertrophic zone, only *Xbp1*$_U$ transcripts were detectable. In *Xbp1*^{CartΔEx2}, most *Xbp1* transcripts in both zones were *Xbp1*$_S$, confirming *in vivo* hyperactivation of IRE1 in *Xbp1*^{CartΔEx2} chondrocytes.

To determine whether IRE1 hyperactivation induces RIDD, we assayed RIDD by qPCR using four established mammalian RIDD marker genes[5]: *Scara3*, *Hgsnat*, *Blos1* and *Pdgfrb*. Firstly, we interrogated primary *Xbp1*^{CartΔEx2} chondrocytes cultured with or without tunicamycin [Fig. 6(B)–(E)], to confirm whether RIDD is induced in *Xbp1*^{CartΔEx2} chondrocytes under ER stress. *Scara3* was significantly downregulated in tunicamycin-treated *Xbp1*^{CartΔEx2} chondrocytes compared to untreated controls. Downregulation of *Hgsnat* ($P = 0.017$) and *Blos1* ($P = 0.053$) was also apparent in tunicamycin-treated *Xbp1*^{CartΔEx2} chondrocytes compared to untreated controls, but only modestly so. This however, is broadly consistent with previous work indicating that the scale of transcript degradation resulting from chemically induced ER stress in mammalian cells is frequently substantially smaller than has been observed in *Drosophila* cells[5]. We could not detect differential expression of *Pdgfrb* in tunicamycin-treated *Xbp1*^{CartΔEx2} chondrocytes compared with untreated controls. Overall however, these results suggest that *Xbp1*^{CartΔEx2} chondrocytes are capable of activating RIDD and degrading target transcripts.

qPCR was performed for our panel of RIDD markers on wildtype or *Xbp1*^{CartΔEx2} proliferative zones [Fig. 6(F)–(I)] as well as wildtype or *Xbp1*^{CartΔEx2} hypertrophic zones [Fig. 6(J)–(M)]. Except for *Blos1* in the hypertrophic zone, we could not detect depletion of any of the transcripts in either growth plate zone from *Xbp1*^{CartΔEx2} compared with the corresponding zone from wildtype. Thus, while *Xbp1*^{CartΔEx2} chondrocytes can induce RIDD, they appear not to do so as a consequence of IRE1 hyperactivation. Therefore, we could exclude RIDD-mediated dysregulation of growth plate gene expression as a factor contributing to the *Xbp1*^{CartΔEx2} phenotype.

Discussion

We analyzed *Xbp1*^{CartΔEx2} mice, in which XBP1 activity is ablated from cartilage. Previous studies involving differentiation of chondrogenic cell lines *in vitro* suggested an essential role for XBP1 in controlling chondrocyte hypertrophy by acting co-ordinately with RUNX2 and regulating *Pthrp*, *Ihh*, *Runx2*, *Col2a1*, and *Col10a1* expression[7]. Our studies show that in the more complex situation of cartilage development *in vivo*, XBP1 is not required for chondrocyte

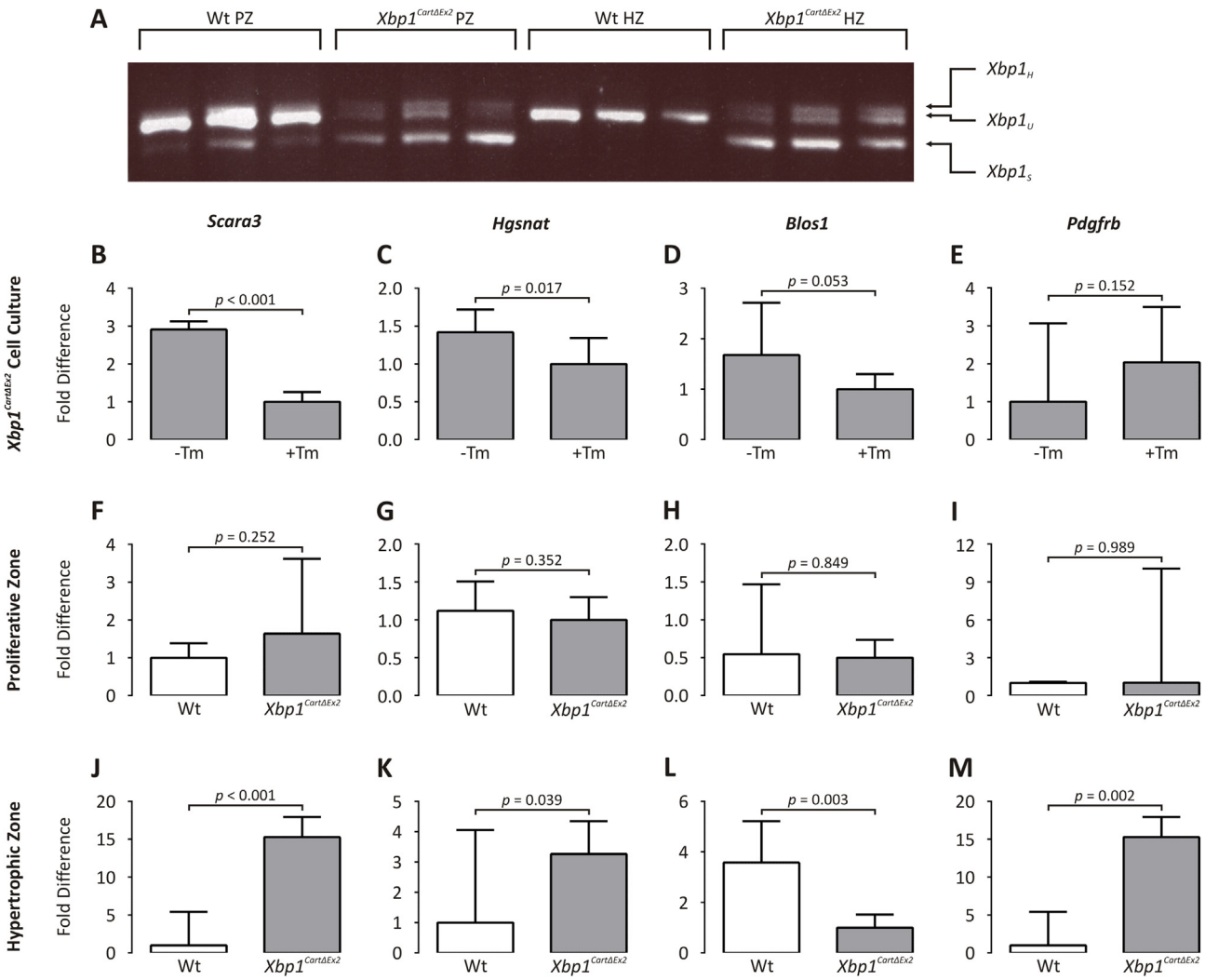

Fig. 6. RIDD is activated in *Xbp1*^{CartΔEx2} chondrocytes in response to ER stress but not IRE1 hyperactivation. (A) RT-PCR performed on cDNA derived from growth plate zones microdissected from two week wildtype (Wt) and *Xbp1*^{CartΔEx2} tibiae to detect the unspliced (*Xbp1*$_U$) and spliced (*Xbp1*$_S$) forms of *Xbp1* in response to ER stress. *Xbp1*$_H$ denotes a heteroduplex product comprised of both *Xbp1*$_U$ and *Xbp1*$_S$ strands. (B–M) qPCR performed using primers specific for (B,F,J) *Scara3*, (C,G,K) *Hgsnat*, (D,H,L) *Blos1*, and (E,I,M) *Pdgfrb*, on cDNA derived from (B,C,D,E) primary *Xbp1*^{CartΔEx2} chondrocytes following culture with (+Tm) or without (−Tm) tunicamycin, (F,G,H,I) microdissected Wt and *Xbp1*^{CartΔEx2} proliferative zones, and (J,K,L,M) microdissected Wt and *Xbp1*^{CartΔEx2} hypertrophic zones. HZ – hypertrophic zone, PZ – proliferative zone.

hypertrophy. Nevertheless, *Xbp1*^{CartΔEx2} exhibits a chondrodysplasia during skeletal development involving disorganized proliferative zone architecture, hypertrophic zone shortening, and delayed mineralization of endochondral bones.

Although we could not detect a significant difference between the length of the proliferative zone in *Xbp1*^{CartΔEx2} and wildtype, the chondrocyte columns of the proliferative zone were significantly longer in the mutant than in wildtype at 2 weeks of age, hinting at a role for the XBP1 pathway in chondrocyte proliferation. This was confirmed by BrdU analysis showing mild impairment of chondrocyte proliferation in the *Xbp1*^{CartΔEx2} growth plate. PTHrP inhibits chondrocyte differentiation and promotes chondrocyte proliferation in the growth plate in a feedback loop involving IHH[24]. Thus, defective IHH/PTHrP signaling could explain the reduced chondrocyte proliferation we observed in the *Xbp1*^{CartΔEx2} growth plate. However, differential expression consistent with reduced chondrocyte proliferation was not detected for key markers of this process, including IHH. The only chondrocyte proliferation marker found to be significantly differentially expressed was *Ccnd1*, which appeared to be modestly upregulated in the mutant proliferative zone. Previous work however, suggests that increased expression of *Ccnd1* in chondrocytes promotes, rather than inhibits their proliferation[22]. Alternatively, our data may point to a role for XBP1 in regulating the activity of integrins or integrin-linked kinase, since disruption to integrin-dependent interactions between chondrocytes and the growth plate matrix are known to result in chondrodysplasias characterized by disrupted proliferative zone architecture[27,28]. Regardless of the precise mechanism involved, our data emphasize for the first time the importance of the XBP1 pathway in regulating the organization and function of growth plate proliferative chondrocytes.

IRE1 was hyperactivated in *Xbp1*^{CartΔEx2} chondrocytes, raising the possibility that the *Xbp1*^{CartΔEx2} phenotype may result from loss of XBP1 activity, IRE1 hyperactivation, or both. A potential consequence of IRE1 hyperactivation in *Xbp1*^{CartΔEx2} is dysregulation of growth plate gene expression through RIDD[5,29]. Analysis of mammalian markers of RIDD[5] revealed that while ER stress is sufficient to trigger RIDD in *Xbp1*^{CartΔEx2} chondrocytes, IRE1 hyperactivation alone is not, excluding RIDD from the *Xbp1*^{CartΔEx2} growth plate pathology. These data also indicate differences in the

activation of IRE1 by ER stress vs hyperactivation, exposing a further layer of complexity in IRE1 activation to that already reported[5].

Xbp1$^{Cart\Delta Ex2}$ chondrocytes activated a UPR in response to ER stress, although a classical UPR was not observed in the *Xbp1*$^{Cart\Delta Ex2}$ growth plate. Intriguingly, *Luman* was upregulated strongly in both the mutant proliferative and hypertrophic zones compared with wildtype. LUMAN is structurally and functionally homologous to ATF6[30], and can upregulate UPR target genes in response to ER stress[31]. The significance of *Luman* upregulation in *Xbp1*$^{Cart\Delta Ex2}$ chondrocytes is unclear. Our work implies however, that it does not depend on classical ER stress. Rather, *Luman* expression may be induced by IRE1 in an XBP1-independent manner following either ER stress or IRE1 hyperactivation.

The chondrodysplasia in *Xbp1*$^{Cart\Delta Ex2}$ mice is mild, involving a generalized delay in endochondral ossification rather than the complete blockage in chondrocyte hypertrophy predicted by recent *in vitro* studies[7]. Indeed, by 7 weeks of age no difference was apparent between wildtype and *Xbp1*$^{Cart\Delta Ex2}$ in terms of the length of endochondral bones or growth plate morphology. This implies a role for XBP1 in regulating the timing of endochondral ossification rather than directing chondrocyte differentiation *per se*. In contrast, the dwarfism phenotype is severe in both the *Bbf2h7* and *Atf4* null mice, due to disrupted protein trafficking and IHH signaling, respectively[2,4]. These differences highlight how endochondral ossification may be regulated by components of ER stress-responsive pathways through a variety of mechanisms.

Finally, we note that activation of XBP1 signaling has been reported as a component of the pathological destruction of cartilage in human and animal models of osteoarthritis (OA)[32,33], a disease characterized by re-activation of chondrocyte proliferation, differentiation and hypertrophy programs[34]. Our work provides links between XBP1 and each of these aspects of chondrocyte biology *in vivo*, by implying that it promotes chondrocyte proliferation and regulates the timing of cartilage maturation and biomineralization. Future studies will address the role of the XBP1 pathway in the pathology of OA by investigating the progression of joint pathology in *Xbp1*$^{Cart\Delta Ex2}$ mice following destabilization of the medial meniscus.

In conclusion, we have demonstrated that XBP1 regulates chondrocyte proliferation and the timing of cartilage maturation and matrix mineralization during endochondral ossification. This study is the first to analyze the function of XBP1 in growth plate cartilage, and extends our understanding of how key UPR components interact with molecular pathways controlling physiological development.

Author contributions

Study design: TLC, ILG, KMB, KAP, RPB-H, LHG, MDB, JFB. Study conduct: TLC, ILG, KMB, CLH, LS, EMS, RW, KAP, JE. Data analysis: TLC, ILG, KMB, KAP, RW, JE, LGH, MDB, JFB. Data interpretation: TLC, ILG, KMB, KAP, JE, LGH, MDB, JFB. Drafting manuscript: TLC, JFB. Approving final version of manuscript: All authors.

Role of funding source

1. This work was funded by the National Health and Medical Research Council of Australia grant #607398 (JFB), the Victorian Government's Operational Infrastructure Support Program, and NIH Grant HD055601 (LHG).
2. These funding sources had no role in study design, collection, analysis or interpretation of data, or writing the manuscript, or decision to submit the manuscript.

Conflict of interest statement

The authors had no financial or personal relationships with people or organizations that could inappropriately bias the presented work.

Acknowledgments

The authors thank Dr Susan Donath (Murdoch Childrens Research Institute, Data Sciences Core) for statistical advice. MDB is the recipient of a Wellcome Trust Senior Research Fellowship in Basic Biomedical Science; Grant 084353/Z/07/Z.

Supplementary data

Supplementary data related to this article can be found at http://dx.doi.org/10.1016/j.joca.2015.01.001.

References

1. Asada R, Kanemoto S, Kondo S, Saito A, Imaizumi K. The signalling from endoplasmic reticulum-resident bZIP transcription factors involved in diverse cellular physiology. J Biochem 2011;149:507–18.
2. Saito A, Hino S, Murakami T, Kanemoto S, Kondo S, Saitoh M, *et al*. Regulation of endoplasmic reticulum stress response by a BBF2H7-mediated Sec23a pathway is essential for chondrogenesis. Nat Cell Biol 2009;11:1197–204.
3. Hetz C. The unfolded protein response: controlling cell fate decisions under ER stress and beyond. Nat Rev Mol Cell Biol 2012;13:89–102.
4. Wang W, Lian N, Li L, Moss HE, Wang W, Perrien DS, *et al*. Atf4 regulates chondrocyte proliferation and differentiation during endochondral ossification by activating Ihh transcription. Development 2009;136:4143–53.
5. Hollien J, Lin JH, Li H, Stevens N, Walter P, Weissman JS. Regulated Ire1-dependent decay of messenger RNAs in mammalian cells. J Cell Biol 2009;186:323–31.
6. Glimcher LH. XBP1: the last two decades. Ann Rheum Dis 2010;69(Suppl 1):i67–71.
7. Liu Y, Zhou J, Zhao W, Li X, Jiang R, Liu C, *et al*. XBP1S associates with RUNX2 and regulates chondrocyte hypertrophy. J Biol Chem 2012;287:34500–13.
8. Hetz C, Lee AH, Gonzalez-Romero D, Thielen P, Castilla J, Soto C, *et al*. Unfolded protein response transcription factor XBP-1 does not influence prion replication or pathogenesis. Proc Natl Acad Sci USA 2008;105:757–62.
9. Ovchinnikov DA, Deng JM, Ogunrinu G, Behringer RR. Col2a1-directed expression of Cre recombinase in differentiating chondrocytes in transgenic mice. Genesis 2000;26:145–6.
10. Lee AH, Scapa EF, Cohen DE, Glimcher LH. Regulation of hepatic lipogenesis by the transcription factor XBP1. Science 2008;320:1492–6.
11. Miller KA, Ah-Cann CJ, Welfare MF, Tan TY, Pope K, Caruana G, *et al*. Cauli: a mouse strain with an Ift140 mutation that results in a skeletal ciliopathy modelling Jeune syndrome. PLoS Genet 2013;9:e1003746.
12. Rajpar MH, McDermott B, Kung L, Eardley R, Knowles L, Heeran M, *et al*. Targeted induction of endoplasmic reticulum stress induces cartilage pathology. PLoS Genet 2009;5:e1000691.
13. Wilson R, Freddi S, Chan D, Cheah KS, Bateman JF. Misfolding of collagen X chains harboring Schmid metaphyseal chondrodysplasia mutations results in aberrant disulfide bond formation, intracellular retention, and activation of the unfolded protein response. J Biol Chem 2005;280:15544–52.

14. Pirog-Garcia KA, Meadows RS, Knowles L, Heinegard D, Thornton DJ, Kadler KE, *et al*. Reduced cell proliferation and increased apoptosis are significant pathological mechanisms in a murine model of mild pseudoachondroplasia resulting from a mutation in the C-terminal domain of COMP. Hum Mol Genet 2007;16:2072–88.
15. Wilson R, Diseberg AF, Gordon L, Zivkovic S, Tatarczuch L, Mackie EJ, *et al*. Comprehensive profiling of cartilage extracellular matrix formation and maturation using sequential extraction and label-free quantitative proteomics. Mol Cell Proteomics 2010;9:1296–313.
16. Cameron TL, Bell KM, Tatarczuch L, Mackie EJ, Rajpar MH, McDermott BT, *et al*. Transcriptional profiling of chondrodysplasia growth plate cartilage reveals adaptive ER-stress networks that allow survival but disrupt hypertrophy. PLoS One 2011;6:e24600.
17. Cameron TL, Belluoccio D, Farlie PG, Brachvogel B, Bateman JF. Global comparative transcriptome analysis of cartilage formation in vivo. BMC Dev Biol 2009;9:20.
18. Belluoccio D, Bernardo BC, Rowley L, Bateman JF. A microarray approach for comparative expression profiling of the discrete maturation zones of mouse growth plate cartilage. Biochim Biophys Acta 2008;1779:330–40.
19. Reimold AM, Grusby MJ, Kosaras B, Fries JW, Mori R, Maniwa S, *et al*. Chondrodysplasia and neurological abnormalities in ATF-2-deficient mice. Nature 1996;379:262–5.
20. James CG, Woods A, Underhill TM, Beier F. The transcription factor ATF3 is upregulated during chondrocyte differentiation and represses cyclin D1 and A gene transcription. BMC Mol Biol 2006;7:30.
21. Beier F, Taylor AC, LuValle P. Activating transcription factor 2 is necessary for maximal activity and serum induction of the cyclin A promoter in chondrocytes. J Biol Chem 2000;275:12948–53.
22. LuValle P, Beier F. Cell cycle control in growth plate chondrocytes. Front Biosci 2000;5:D493–503.
23. Long F, Ornitz DM. Development of the endochondral skeleton. Cold Spring Harb Perspect Biol 2013;5:a008334.
24. Kronenberg HM. PTHrP and skeletal development. Ann N Y Acad Sci 2006;1068:1–13.
25. St-Jacques B, Hammerschmidt M, McMahon AP. Indian hedgehog signaling regulates proliferation and differentiation of chondrocytes and is essential for bone formation. Genes Dev 1999;13:2072–86.
26. Lee AH, Heidtman K, Hotamisligil GS, Glimcher LH. Dual and opposing roles of the unfolded protein response regulated by IRE1alpha and XBP1 in proinsulin processing and insulin secretion. Proc Natl Acad Sci USA 2011;108:8885–90.
27. Grashoff C, Aszodi A, Sakai T, Hunziker EB, Fassler R. Integrin-linked kinase regulates chondrocyte shape and proliferation. EMBO Rep 2003;4:432–8.
28. Aszodi A, Hunziker EB, Brakebusch C, Fassler R. Beta1 integrins regulate chondrocyte rotation, G1 progression, and cytokinesis. Genes Dev 2003;17:2465–79.
29. Hollien J, Weissman JS. Decay of endoplasmic reticulum-localized mRNAs during the unfolded protein response. Science 2006;313:104–7.
30. Raggo C, Rapin N, Stirling J, Gobeil P, Smith-Windsor E, O'Hare P, *et al*. Luman, the cellular counterpart of herpes simplex virus VP16, is processed by regulated intramembrane proteolysis. Mol Cell Biol 2002;22:5639–49.
31. DenBoer LM, Hardy-Smith PW, Hogan MR, Cockram GP, Audas TE, Lu R. Luman is capable of binding and activating transcription from the unfolded protein response element. Biochem Biophys Res Commun 2005;331:113–9.
32. Bateman JF, Rowley L, Belluoccio D, Chan B, Bell K, Fosang AJ, *et al*. Transcriptomics of wild-type mice and mice lacking ADAMTS-5 activity identifies genes involved in osteoarthritis initiation and cartilage destruction. Arthritis Rheum 2013;65:1547–60.
33. Takada K, Hirose J, Senba K, Yamabe S, Oike Y, Gotoh T, *et al*. Enhanced apoptotic and reduced protective response in chondrocytes following endoplasmic reticulum stress in osteoarthritic cartilage. Int J Exp Pathol 2011;92:232–42.
34. Goldring MB. Chondrogenesis, chondrocyte differentiation, and articular cartilage metabolism in health and osteoarthritis. Ther Adv Musculoskelet Dis 2012;4:269–85.